

Article

A Novel Prediction Approach for Short-Term Renewable Energy Consumption in China Based on Improved Gaussian Process Regression

Yuansheng Huang ¹, Lei Yang ^{1,*} , Chong Gao ², Yuqing Jiang ² and Yulin Dong ²

¹ School of Economics and Management, North China Electric Power University, Beijing 102206, China; hys2656@aliyun.com

² School of Economics and Management, North China Electric Power University, Baoding 071003, China; 51851114@ncepu.edu.cn (C.G.); 2182218063@ncepu.edu.cn (Y.J.); 2182218022@ncepu.edu.cn (Y.D.)

* Correspondence: 1162106026@ncepu.edu.cn; Tel.: +86-186-317-28689

Received: 9 September 2019; Accepted: 30 October 2019; Published: 1 November 2019



Abstract: Energy consumption issues are important factors concerning the achievement of sustainable social development and also have a significant impact on energy security, particularly for China whose energy structure is experiencing a transformation. Construction of an accurate and reliable prediction model for the volatility changes in energy consumption can provide valuable reference information for policy makers of the government and for the energy industry. In view of this, a novel improved model is developed in this article by integrating the modified state transition algorithm (MSTA) with the Gaussian processes regression (GPR) approach for non-fossil energy consumption predictions for China at the end of the 13th Five-Year Project, in which the MSTA is utilized for effective optimization of hyper-parameters in GPR. Aiming for validating the superiority of MSTA, several comparisons are conducted on two well-known functions and the optimization results show the effectiveness of modification in the state transition algorithm (STA). Then, based on the latest statistical renewable energy consumption data, the MSTA-GPR model is utilized to generate consumption predictions for overall renewable energy and each single renewable energy source, including hydropower, wind, solar, geothermal, biomass and other energies, respectively. The forecasting results reveal that the proposed improved GPR can promote the forecasting ability of basic GPR and obtain the best prediction effect among all the other comparison models. Finally, combined with the forecasting results, the trend of each renewable energy source is analyzed.

Keywords: renewable energy consumption; Gaussian processes regression; state transition algorithm; five-year project; forecasting

1. Introduction

The energy industry provides an important impetus for the advancement of society and has a significant impact on sustainable development [1–5], power safety [6,7], and environmental changes [8,9]. Aiming to alleviate the pressure brought by energy problems, developing renewable energy has been considered as an effective approach by more and more scholars at home and abroad [10]. In China, renewable energies refer to the energies that can be continuously regenerated in nature, for instance, hydropower, wind, solar, biomass, geothermal and so on. The latest statistics obtained from British Petroleum (BP) Statistical Review of World Energy 2019 displays that the renewable energy consumption in China has reached the amount of 391.67 million tons oil equivalent (Mtoe), which experienced a huge promotion over the past decades. China's overall non-fossil energy consumption in 2018 increased 8.1% compared with that of 2017. During the past year, the hydropower

has promoted by 3.2%, the wind energy consumption has increased by 24.1%, the solar energy consumption has grown by 50.7%, and geothermal, biomass and other energy has been promoted by 14%. According to the collected data, the consumption and the corresponding proportion of different renewable energies in the past ten years are exhibited in Figure 1.

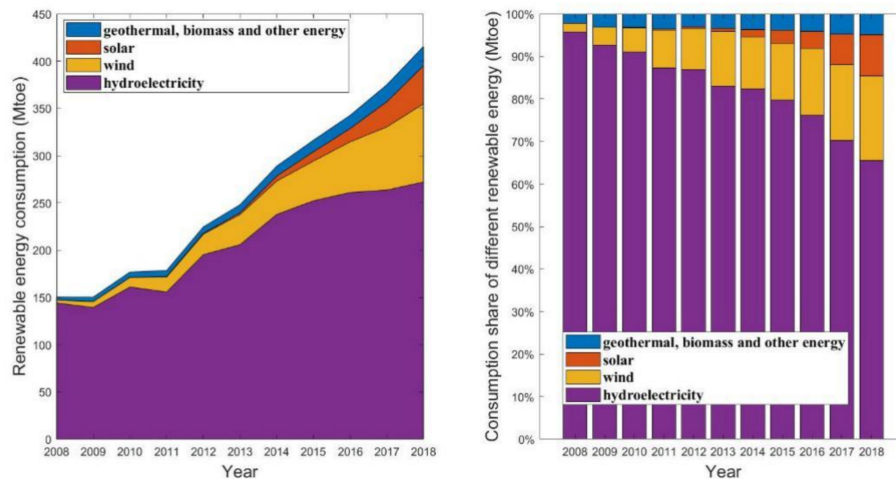


Figure 1. The composition of renewable energy consumption in China.

As displayed in Figure 1, dramatic changes can be observed in the composition of non-fossil energy consumption of China during the past few years owing to a series of incentive policies implementations, especially during the twelfth Five-Year Project which was from 2011 to 2015. Hydropower, with the consumption of 144.1 Mtoe, accounts for 95.77% of the overall renewable energy consumption in 2008. However, due to the development of other renewable energies, the share of hydropower has fallen to 79.73% during the late years of the twelfth Five-Year Project, and further decreased to 69.47% by the year-end of 2018. Meanwhile, the wind energy accounts for the biggest growth share in renewable consumption, which increased from 1.97% in 2008 to 10.93% in 2018, and the corresponding consumption amount increased from 2.96 Mtoe to 82.82 Mtoe. The share of solar energy in the overall renewable consumption grew from 0.02% in 2008 to 9.66% in 2018, with the corresponding growth from 0.03 Mtoe to 40.16 Mtoe. The share of geothermal, biomass and other energy consumption in the overall renewable consumption grew from 2.24% in 2008 to 4.94% in 2018, with the corresponding growth from 3.37 Mtoe to 20.53 Mtoe. Presently, aiming at realizing sustainable development, China is focusing on modifying the traditional energy supply structure dominated by fossil fuels and encouraging the utilization of non-fossil energy in power generation. Thus, the establishment of a reliable and accurate foreseeing for China's non-fossil energy consumption at the end of thirteenth Five-Year Project (2016–2020) and afterwards is of practical significance, offering valuable references to contribute for the healthy and steady growth of China's energy and economy.

In aiming for obtaining a satisfactory forecasting performance, a number of approaches have been developed to predict energy consumption, for instance: time series analysis [11], the Long-range Energy Alternatives Planning System (LEAP) [12,13], the Nanoelectromechanical systems approach (NEMS) [14,15], computational intelligence technology [16] and hybrid forecasting systems [17,18]. However, although the models listed above have strong non-linear modeling ability, they cannot capture the characteristics of small-scale samples very well. Aiming to solve this problem, Gaussian process regression is developed as the perfect intelligence approach for low-dimensional and small sample regression problems [19].

Owing to the properties of flexibility, non-linearity, inherent non-parametric factors, and so on, GPR has been utilized by numerous scholars in various fields including chemistry [20], astrophysics [21], materials [22], and so on. For example, estimation of diffusion coefficients in the voltammetric signals was obtained by Bogdan et al., [23] with the application of GPR which is utilized to analyze the

electroanalytical experimental data. In aiming to forecast the export content of the flue gas, GPR was conducted to obtain the design optimization of combustion systems utilizing real time flame figures in [24]. Furthermore, there are also researches involving GPR in the prediction of wind speed [25]. Wang et al. [26] proposed a hybrid approach which combines four different models including Extreme Learning Machine, Support Vector Machine, Least Squares Support Vector Machine and GPR to gain the probabilistic predictions for wind speed in the short term. Based on the features of renewable energy consumption, it is appropriate to utilize GPR for the acquirement of renewable energy consumption prediction. Nevertheless, through the review of the previous studies, it can be noticed that few researches have been investigated in this domain by now.

In the construction of GPR, the choice of hyper-parameters is of great influence on the forecasting capacity. Thus, it is of extreme significance to find a proper value for the hyper-parameter of GPR. As a traditional measure, the conjugate gradient (CG) has been conducted as the optimization operator for parameters selection [27]. Nevertheless, the performance of this measure is affected by the basic guess selection, and it is hard to determine the proper iteration amount. Furthermore, in most instances, the estimation of hyper-parameters for GPR is a non-convex issue, where measures on basis of the gradient have troubles in finding the global optimal value [28,29]. To aim at solving this problem, intelligent optimization measures, including the particle swarm optimization (PSO) [30–32] and the genetic algorithm (GA) [33–35], are found to be better choices for optimal parameters selection in model training process. Among these models mentioned, it is validated that the state transition algorithm (STA) is effective in numerous complicated optimization issues and shows wonderful ability for nonlinear optimization in contrast with GA and PSO [36]. However, the original STA utilizes the space framework of objective function and seeks the best answers with the application of its unique state transformation operators. Additionally, the seeking range of state transformation operators is primarily decided by the corresponding transformation factors. If the transformation factor takes a large value, the global search ability of the model will be stronger. Conversely, as the value of the transformation factor is small, the local search ability of the model will be better. The transformation factor in the traditional structure of STA often takes an invariant value, which will add extra computations in the later period of optimization and cannot contribute for the optimization result improvement. Aiming for calculation complexity reduction and optimization result promotion, it is needed to consider parameter optimization for the transformation factor to find harmony between the global search and local search for the basic STA.

According to the analysis above, in this paper, a GPR model integrated with modified STA is put forward to make predictions of China's overall renewable energy consumption and its respective components consumption. In the proposed model, the parameter selection for STA and the parameter optimization for GPR are considered at the same time. Additionally, the latest renewable energy consumption data published by the BP statistical Review of World Energy 2019 are utilized to test the proposed model. The prediction outcomes prove that the proposed modified state transition algorithm (MSTA)-GPR model displays the optimal prediction effect in contrast with all the other prediction approaches. The major contributions can be described as follows: (1) A novel integration forecasting model MSTA-GPR model is proposed. The MSTA is integrated into the GPR for the hyper-parameters optimization to improve the forecasting performance. (2) Two well-known functions are utilized to validate the optimization effect against traditional optimization algorithms, such as GA and PSO. (3) The proposed MSTA-GPR is utilized to make consumption predictions of China's renewable energy at the end of the thirteenth Five-Year Project. The final result proves the satisfactory forecasting performance of the MSTA-GPR model and provides both a deterministic and an interval prediction for the renewable energy consumption development.

This passage is arranged with the following framework: Section 2 provides the description of the GPR, MSTA and the proposed MSTA-GPR model; Section 3 provides two validation cases to test the optimization performance of the modification in the basic STA; Section 4 shows applications of the

proposed MSTA-GPR model for the consumption prediction of the overall renewable energy and its corresponding components; finally, the conclusions are obtained in Section 5.

2. Methodology

2.1. Gaussian Process Regression

Gaussian process (GP) is a kind of stochastic process in probability theory and mathematical statistics. It is a combination of a series of random variables obeying normal distribution in an exponential set. GP has two important components, one is the average function, and the other is the covariance function, which can describe the GP in form of Equation (1).

$$f(x) \sim GP(a(x), C(x, x')) \quad (1)$$

The form of average function is described in Equation (2), and the form of covariance equation is represented by Equation (3) [37].

$$a(x) = E[f(x)], \quad (2)$$

$$C(x, x') = E[(f(x) - a(x))(f(x') - a(x'))]. \quad (3)$$

Generally, the squared-exponential covariance equation is considered as a widely applied covariance function. Assume that there is a data set with noise for training, which is in form of Equation (4):

$$D = \{x^{(i)}, y^{(i)} \mid i = 1, 2, \dots, n\} \quad (4)$$

then, we apply the GPR method to make predictions for the output value of y^* with the future input value x^* in way of studying a function from the data set given, which relates to a presupposed prior Gaussian function.

The posterior distribution can be acquired for the $(n + 1)$ GP results according to Bayes rule, when the distribution for a novel value is calculated. As an examination input x^{n+1} and the corresponding training set D are given, the forecasting outcomes follow normal distribution by adjusting the observed values of the training set, which is shown from Equation (4) to Equation (6).

$$P(y^{(n+1)} \mid D, x^{(n+1)}) \sim N(\mu_{y^{(n+1)}}, \sigma_{y^{(n+1)}}^2), \quad (4)$$

$$\mu_{y^{(n+1)}} = a^T Q^{-1} y, \quad (5)$$

$$\sigma_{y^{(n+1)}}^2 = C(x^{(n+1)}, x^{(n+1)}) - \alpha^T Q^{-1} \alpha. \quad (6)$$

In the above equations, $\mu_{y^{(n+1)}}$ represents the mean, and $\sigma_{y^{(n+1)}}^2$ means the variance. Q_{pq} and α_p are given in equations below:

$$Q_{pq} = C(x^{(p)}, x^{(q)}) + r^2 \theta_{pq}, \quad (7)$$

$$\alpha_p = C(x^{(n+1)}, x^{(q)}), p = 1, 2, \dots, n. \quad (8)$$

Mentioned by the previous paragraphs, covariance function $C(x_p, x_q; \Theta)$ along with hyper-parameters Θ has a great effect in GPR as it decides the smoothness of the data in evaluating the new function. As mentioned in [38], the log likelihood can be maximized to choose the optimal hyper-parameters for GPR, which is described in Equation (9):

$$\begin{aligned} \log P(D \mid \Theta) &= \log P(y^{(1)}, y^{(2)}, \dots, y^{(n)} \mid x^{(1)}, x^{(2)}, \dots, x^{(n)}, \Theta) \\ &= -\frac{1}{2} \log \det C - \frac{1}{2} y^T C^{-1} y - \frac{n}{2} \log 2\pi \end{aligned} \quad (9)$$

2.2. Improved State Transition Algorithm

2.2.1. Original State Transition Algorithm

Firstly, an equation to be optimized with no limitations is described as follow:

$$\min_{x \in R^n} f(x) \quad (10)$$

where, $f(x)$ denotes an objective function mapping from R^n to R . Assume the potential solution as a state, and the objective problem is solved through updating the optimal solution found by now with iterations, which is considered as state transition. The procedure of STA is expressed as below:

$$\begin{cases} s_{k+1} = A_k s_k + B_k u_k \\ y_{k+1} = f(s_{k+1}) \end{cases} \quad (11)$$

where, a state is represented by s_k ; the state transition matrices are represented by A_k and B_k ; the function of s_k and the previous states are represented by u_k ; and the objective function is described utilizing the symbol of f . Additionally, the solutions of the continuous objective function of the STA are searched for with four different state transformation operators below.

(1) Rotation transformation:

$$s_{k+1} = s_k + \alpha \frac{1}{n \|s_k\|_2} R_r s_k \quad (12)$$

where, the rotation factor is positive and represented by α . A random matrix which belongs to $R^{n \times n}$ is denoted by R_r with elements distributed in $[-1,1]$. $\|\times\|$ defines the L2-norm of a vector. Utilization of the rotation transformation can contribute to the search in the hypersphere.

(2) Translation transformation:

$$s_{k+1} = s_k + \beta R_t \frac{s_k - s_{k-1}}{\|s_k - s_{k-1}\|_2} \quad (13)$$

where, the translation factor is a fixed positive value and represented by β . R_t belonging to R defines a stochastic variable and the corresponding elements of R_t take value between $[0,1]$. Application of the translation transformation can contribute to the line search along between x_{k-1} and x_k .

(3) Expansion transformation:

$$s_{k+1} = s_k + \gamma R_e x_k \quad (14)$$

where, the expansion factor is a fixed positive value which is represented by γ . A stochastic diagonal matrix is represented by $R_e \in R^{n \times n}$ with elements obeying normal distribution. Application of expansion transformation can contribute to the whole space search which spreads the element in x_k to the range of infinite.

(4) Axesion transformation:

$$s_{k+1} = s_k + \delta R_a x_k \quad (15)$$

where, the axesion factor is a fixed positive value and defined by δ ; a stochastic diagonal matrix which is represented by $R_a \in R^{n \times n}$ with elements generated from normal distribution. Moreover, there is only one nonzero stochastic element in R_a . Utilization of the axesion transformation can contribute to the search along the direction of axes.

Furthermore, the search enforcement (SE) is a parameter which is utilized to control the amount of each transformation during the implementation of four different transformation operators.

The major steps of the basic STA can be described as follow [39]:

- 1: repeat
- 2: repeat if $\alpha < \alpha_{\min}$ then
- 3: $\alpha \leftarrow \alpha_{\min}$
- 4: end if
- 5: $Optimal \leftarrow expansion(fun, Optimal, SE, \beta, \gamma)$
- 6: $Optimal \leftarrow rotation(fun, Optimal, SE, \alpha, \beta)$
- 7: $Optimal \leftarrow axesion(fun, Optimal, SE, \beta, \delta)$
- 8: $\alpha \leftarrow \frac{\alpha}{fc}$

where, lessening of the coefficient α is decided by fc which takes a fixed value. Once a better solution is found, the translation operator will be activated.

2.2.2. Modification for the Original State Transition Algorithm

Compared with models on basis of the gradient, the STA has one advantage which is to search in all orientations and at any length. But there are also limitations for the STA. For example, decided by the transformation factor, the search area of the rotation and translation transformation is limited in a hypersphere or a line. To improve this situation, a parameter set $\Omega = \{1, 10^{-1}, 10^{-2}, 10^{-3}, 10^{-4}, 10^{-5}, 10^{-6}, 10^{-7}, 10^{-8}\}$ is considered in the basic STA for the optimal value selection of transformation factor [40]. The parameter which can obtain the best value for the objective function is selected as the optimal parameter. The optimal parameter \tilde{a}^* is given as the equation below:

$$\tilde{a}^* = \underset{\tilde{a} \in \Omega}{\operatorname{argmin}} f(x_k + \tilde{a}_k \tilde{d}_k). \quad (16)$$

Aiming for a more complete utilization of the parameters, each parameter chosen is held for a certain period, which is represented as T_p . Then the rotation function in the modified STA is described as follow:

- 1: $[Optimal, \alpha] \leftarrow update_alpha(fun, Optimal, SE, \Omega)$
- 2: for $i \leftarrow 1, T_p$ do
- 3: $Optimal \leftarrow rotation(fun, Optimal, SE, \alpha)$
- 4: end for

where, the realization of optimal parameter selection for the rotation factor is conducted by equation update alpha. In this way, the common periodical reduction of the transformation factors is abandoned. The parameter to be optimized is chosen for each state transformation with the exception of the translation operator and the best parameter selected is held within a certain period.

2.2.3. Prediction Process of Improved GPR on Basis of Modified STA (MSTA-GPR)

Three steps are carried out to realize the proposed MSTA-GPR model: Step 1. Initialization; Step 2. The selection of optimal hyper-parameters. The description of the fitness function is shown as Equation (9); Step 3. Forecasting. The flowchart of MSTA-GPR is shown in Figure 2.

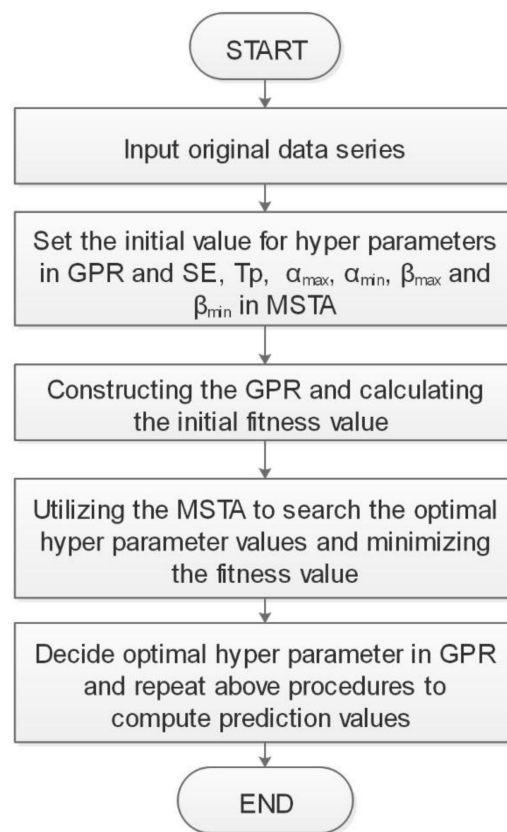


Figure 2. The implementation steps of the proposed modified state transition algorithm-Gaussian processes regression model (MSTA-GPR).

The details of each step are described as follow:

- Step 1. (Initialization): The training set is built to form the input and the covariance function is selected for GPR.
- Step 2. (Selection of optimal hyper-parameters):
 - Step 2.1. Parameter setting: A random initial solution $Optimal_0$ is created in the searching space. Parameters for MSTA are set: $\alpha = \alpha_{max}, \alpha_{min}$, $\beta = \beta_{max}, \beta_{min}$, γ , T_p , fun , and SE. The max function estimations are set to $5e4 * n * \log(n)$ and n is the amount of the decision variables.
 - Step 2.2. Expansion: Create SE potential solutions with the expansion transformation operator on basis of the optimal solution $Optimal_k$ found so far. Renew the optimal solution when $Optimal_k$ is promoted. After that, translation transformation operator is applied and the optimal solution is renewed; otherwise not.
 - Step 2.3. Rotation: Create SE potential solutions with the rotation transformation operator on basis of the optimal solution $Optimal_k$ found so far. Renew the optimal solution when $Optimal_k$ is promoted. After that, the translation transformation operator is applied and the optimal solution is renewed; otherwise not.
 - Step 2.4. Optimal parameter selection for STA: the optimal transformation factors are selected for STA according to the description in Section 2.2.2.
 - Step 2.5. Termination: If α or β is beyond the upper or lower bound, they will be set as the corresponding value of the upper or lower bound. The iteration continues until the corresponding termination is achieved. Thus, the optimal hyper-parameters of GPR are found.

Step 3. (Prediction): The new data are introduced to form the corresponding input of the MSTA-GPR model for prediction. Finally, the forecasting results are obtained.

3. Validation of MSTA Optimization

In this section, the global optimization ability of MSTA is investigated with two famous equations, which can validate the effectiveness of the modification in basic STA. The test equations are shown as follow:

(1) Rosenbrock function:

$$f_1 = \sum_{i=1}^n (100(x_{i+1} - x_i^2)^2 + (x_i - 1)^2). \quad (17)$$

The constrain for the equation above is $x_i \in [0, \pi], i = 1, 2, \dots, n$. The optimal solution is $x_{op} = (0, \dots, 0)$ and the corresponding optimal value for the function is 0.

(2) Michalewicz function:

$$f_2 = -\sum_{i=1}^n \sin(x_i) \sin\left(\frac{ix_i^2}{\pi}\right)^{20}. \quad (18)$$

The constrain for the equation above is that $x_i \in [0, \pi], i = 1, 2, \dots, n$. And the corresponding optimal value for the equation is not known.

The basic STA and two widely used optimization approaches, which are PSO and GA, are utilized to form comparisons for MSTA. The corresponding parameter setting recommended for the algorithms involved are shown in Table 1. The dimension for decision variable is investigated at 20, 30, and 50. Aiming for comparisons in the same situation, all programs are coded in Matlab 2018a on a personal computer with 8 GB RAM under a Windows environment and the computation procedures are conducted 20 times.

Table 1. Parameter setting for each optimization model involved. GA, genetic algorithm; PSO, particle swarm optimization.

Prediction Approaches	Parameter	Value
MSTA	SE	20
	T_p	10
	Range	$[10^{-3} \times \text{Dim}, 1000 \times \text{Dim}]$
STA [36]	SE	20
	Rotation factor scope	$[10^{-4}, 1]$
	Translation factor	1
	Expansion factor	1
	Axesion factor	1
GA [41]	Population	20
	Crossover rate	0.95
	Tournament size	2
	Mutation rate	0.05
PSO [42]	Swarm size	30
	Inertia range	$[0.1, 1.1]$
	Self-adjustment weight	1.49
	Social-adjustment weight	1.49
	Minimum neighborhood size	$0.25 \times \text{swam size}$

It can be known from Table 2 that, in the case of the Rosenbrock function, the optimization performance of MSTA is validated to be the best compared with the other three comparison optimization algorithms regardless of the best, worst, or mean situation. And even as the dimension of the independent variable increases, the MSTA can still achieve a satisfactory result which is superior to

the optimization outcomes of STA, GA, or PSO. Moreover, in the case of the Michalewicz function, as the global optimal solution is not known, the optimization capacity of each algorithm can be better explored one step further on. It can still be seen that from Table 2, the optimal outcomes obtained by MSTA are the best among all the optimization algorithms under different situations and dimensions, which again proves the superiority of MSTA optimization. For example, when the dimension takes 20, compared with STA, GA, and PSO, the mean optimal value promotion of MSTA is 8.15%, 9.94% and 97.32%, respectively. Conclusively, the two validation cases show the effectiveness of the modification for the basic STA. Integrated with the optimal parameter selection, the performance of MSTA is thus improved significantly and is better than that of the basic STA and the two traditional optimal algorithms, which makes it a better choice for hyper parameter optimization in GPR.

Table 2. Validation comparisons of different optimization algorithms.

Fun	Dim	f_1			f_2		
		20	30	50	20	30	50
MSTA	Best	6.06×10^{-7}	8.40×10^{-7}	1.84×10^{-6}	-19.96	-29.95	-49.97
	Worst	1.10×10^{-6}	1.88×10^{-6}	2.87×10^{-6}	-19.78	-29.87	-49.93
	Mean	8.03×10^{-7}	1.26×10^{-6}	2.16×10^{-6}	-19.91	-29.91	-49.95
STA	Best	11.17	23.75	36.91	-19.60	-29.53	-49.39
	Worst	13.57	24.66	45.34	-17.60	-27.51	-46.51
	Mean	12.94	24.10	42.34	-18.41	-28.82	-47.85
GA	Best	0.49	0.04	0.08	-18.11	-28.86	-41.26
	Worst	0.49	0.04	0.08	-18.11	-28.86	-41.26
	Mean	0.49	0.04	0.08	-18.11	-28.86	-41.26
PSO	Best	13.26	1.48	13.24	10.09	-15.76	-7.97
	Worst	13.26	1.48	13.24	10.09	-15.76	-7.97
	Mean	13.26	1.48	13.24	10.09	-15.76	-7.97

4. Application of MSTA-GPR for Overall Renewable Energy Consumption Prediction in China

In this Section, the MSTA-GPR approach is applied for the renewable energy consumption prediction in China. Aiming for validation of the superiority of MSTA-GPR approach, the corresponding forecasting results are compared with that of PSO-GPR [43], GPR [44] and the autoregressive integrated moving average ARIMA model [45]. The basic data are offered by the BP statistical Review of World Energy 2019. The training set is formed utilizing observations obtained from 2008 to 2015 to train each forecasting model involved, and the first three years of the thirteenth Five-Year Project (2016–2020) are considered to validate the corresponding prediction effect. All the original data are listed in Table 3.

Table 3. The consumption data for China's renewable energy from 2006 to 2018.

Year	Overall	Hydropower	Wind	Solar	Geothermal Biomass and Other
2006	101.08	98.61	0.84	0.02	1.61
2007	113.30	109.80	1.24	0.03	2.23
2008	150.49	144.13	2.96	0.03	3.36
2009	150.33	139.30	6.25	0.06	4.72
2010	176.86	160.97	10.10	0.16	5.63
2011	178.46	155.69	15.91	0.59	6.27
2012	224.66	195.23	21.72	0.81	6.90
2013	248.10	205.82	31.95	1.89	8.44
2014	288.99	237.85	35.32	5.32	10.50
2015	316.31	252.19	42.03	9.86	12.23
2016	342.62	260.96	53.64	13.96	14.06
2017	375.04	263.63	66.75	26.65	18.01
2018	415.59	272.08	82.82	40.16	20.53

Besides, aiming for the prediction performance evaluation, the mean absolute percent error (MAPE) is computed for the forecasting outcome of each model involved. The equation of MAPE is described as follow:

$$MAPE = \frac{1}{Y} \sum_{y=1}^Y \left| \frac{p^{true}(y) - p^{forecast}(y)}{p^{true}(y)} \right| \times 100\% \tag{19}$$

where, $p^{true}(y)$ means the data recorded at year y , $p^{forecast}(y)$ means the prediction of year y , and Y is the amount of all the values to be predicted.

4.1. Overall Renewable Energy Consumption

The suggested MSTA-GPR approach is utilized in this part to investigate the overall renewable energy consumption prediction in China. The predictions and corresponding indexes are displayed in Table 4. Figure 3 displays the interval prediction for the overall renewable energy consumption in China from 2016 to 2018. And in the interval prediction, the 95% upper bound and the 95% lower bound reveal the maximum values and minimum values respectively that can be obtained by GPR when the confidence level of the regression prediction result is 95%.

Table 4. Consumption prediction for overall renewable energy of China from 2006 to 2018 (Mtoe). ARIMA, autoregressive integrated moving average; MAPE, mean absolute percent error.

Year	Real Data	MSTA-GPR		PSO-GPR		GPR		ARIMA	
		Value	Error (%)	Value	Error (%)	Value	Error (%)	Value	Error (%)
2016	342.62	347.08	1.30	348.39	1.68	348.88	1.83	343.72	0.32
2017	375.04	375.04	0.00	374.40	0.17	374.70	0.09	371.17	1.03
2018	415.59	405.29	2.48	401.07	3.49	400.94	3.53	398.66	4.07
MAPE			1.26		1.78		1.81		1.81

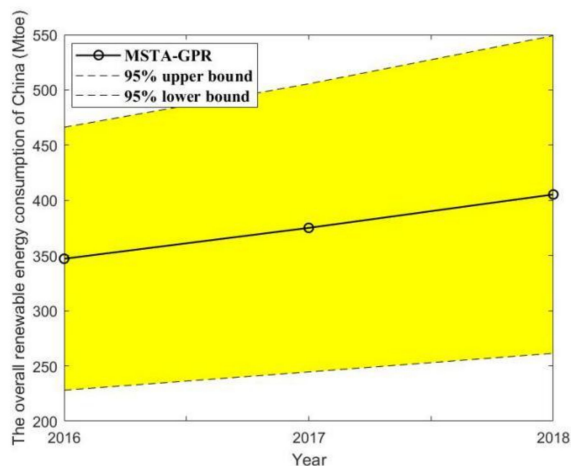


Figure 3. The interval prediction result of MSTA-GPR for overall renewable energy consumption in China.

From Table 4 and Figure 3, it can be observed that the prediction outcomes reveal that the MSTA-GPR approach offers a more satisfactory forecasting accuracy than the other approaches in consumption predicting of the overall renewable energy in China. It can be obtained from the historical data that in recent years, the development of China’s overall renewable energy consumption is close to linear growth. Hence, GPR and ARIMA have similar prediction performance. Compared with GPR and ARIMA, the MSTA-GPR approach has promoted each forecasting accuracy by 30.39%. Optimized by PSO, the prediction performance of PSO-GPR is slightly better than that of basic GPR. Compared with PSO-GPR, the MSTA-GPR approach has promoted the forecasting accuracy by 29.21%. This comparison result indicates that the global ability of MSTA is better than that of PSO. As can

be seen from Table 4, the trend of overall renewable energy consumption in China keeps growing in the last few years and will continue to maintain in the future. According to the latest published statistics, by the first half of 2019, the amount of electricity generated by renewable energy has reached 887.9 billion kWh, which increases 14% compared with that of last year.

4.2. Hydroelectricity Consumption in China

This part investigates the prediction of China's hydroelectricity consumption. The prediction outcomes of each model and corresponding errors are displayed in Table A1 of Appendix A. Furthermore, the interval prediction for China's hydroelectricity consumption is described in Figure A1 of Appendix A.

From Table A1 and Figure A1, it can be observed that the prediction outcomes reveal that the MSTA-GPR approach offers a more satisfactory forecasting performance than the other approaches in predicting the hydroelectricity consumption of China. As can be obtained from the historical data, the growth trend of hydroelectricity is not continuous. The forecasting performance of ARIMA is the worst of all. Compared with ARIMA, the MSTA-GPR approach has promoted the forecasting accuracy by 91.08%. GPR offers a better forecasting result than that of ARIMA by recognizing the non-linear features in the historical data. However, the prediction performance of GPR is not the best because the hyper-parameters are not optimized. Compared with GPR, the MSTA-GPR approach has promoted the forecasting accuracy by 66.67%. Combined with PSO, the forecasting accuracy of PSO-GPR is further promoted than basic GPR. But PSO is easy to fall into the local optimum in the process of searching the optimal solution. Compared with PSO-GPR, the MSTA-GPR approach has promoted the forecasting accuracy by 29.54%. In recent years, the growth rate of hydropower has slowed down, but still accounts for the largest proportion of renewable energy consumption in China. The latest published statistics shows that, by the first half year of 2019, the amount of electricity generated by hydropower is 513.8 billion kWh, which has promoted by 11.8% compared with that of last year.

4.3. Wind Power Consumption in China

This Section explores the prediction of China's wind power consumption. Prediction outcome of each model and corresponding errors are displayed in Table A2 of Appendix A. Additionally, the interval prediction for China's wind power consumption is described in Figure A2 of Appendix A.

From Table A2 and Figure A2, it can be observed that the prediction outcomes reveal that the MSTA-GPR approach offers a more satisfactory forecasting performance than the other approaches in predicting the wind power consumption of China. According to historical data, the consumption of wind power has increased rapidly in recent years. As a traditional time series forecasting method, ARIMA cannot capture the nonlinear growth trend of wind power consumption well, which results in a poor forecasting result. Compared with ARIMA, the MSTA-GPR approach has promoted the forecasting accuracy by 36.81%. Owing to the advantage of recognizing non-linear features in data, both PSO-GPR and GPR can obtain better forecasting results than ARIMA. However, due to the lack of a more effective hyper parameter optimization method, their forecasting performances are not good as that of MSTA-GPR. Compared with PSO-GPR and GPR, the MSTA-GPR approach has promoted the forecasting accuracy by 7.98% and 25.07%, respectively. In recent years, with the gradual maturity of technology, wind power generation has been vigorously developed, and the amount generated by wind power is increasing year by year. By the first half year of 2019, the wind power generation in China has achieved 214.5 billion kWh, which has promoted by 11.5% compared with that of last year.

4.4. Solar Power Consumption in China

The solar power consumption prediction of China is investigated in this Section utilizing the MSTA-GPR approach. The prediction outcomes of each model and corresponding errors are displayed in Table A3 of Appendix A. Additionally, the interval prediction for China's solar power consumption is described in Figure A3 of Appendix A.

From Table A3 and Figure A3, it can be observed that the prediction outcomes reveal that the MSTA-GPR approach offers a more satisfactory forecasting performance than the other approaches in predicting the solar power consumption of China. The solar power consumption experiences a rapid growth in recent years. But ARIMA cannot follow the rapid changes of solar power consumption, which results in a low prediction accuracy. Compared with ARIMA, the MSTA-GPR approach has promoted the forecasting accuracy by 63.15%. In contrast, PSO-GPR and GPR can adapt to the rapid changes of solar power consumption in the short term and get better prediction results. But their forecasting accuracy is not the best. Compared with PSO-GPR and GPR, the MSTA-GPR approach has promoted the forecasting accuracy by 0.58% and 29.89%, respectively. With the implementation of the renewable energy incentive policy, solar power generation has been vigorously promoted, and its proportion in renewable energy consumption has also increased year by year. According to the latest data published, by the first half year of 2019, the solar power generation has reached 106.7 billion kWh, which has promoted by 30% compared with that of last year.

4.5. Geothermal, Biomass and Other Energy Consumption Prediction in China

This Section explores the predictions of China's geothermal, biomass and other energy consumption. The prediction outcomes of each model and corresponding errors are displayed in Table A4 of Appendix A. Additionally, the corresponding interval prediction is described in Figure A4 of Appendix A.

From Table A4 and Figure A4, it can be observed that the prediction outcomes reveal that the MSTA-GPR approach offers a more satisfactory forecasting performance than the other approaches in predicting the geothermal, biomass and other types of energy consumption of China. Compared with PSO-GPR, GPR and ARIMA, the MSTA-GPR approach has promoted the forecasting accuracy by 1.94%, 20.98% and 67.49%, respectively. The results show that, compared with the other models, the proposed MSTA-GPR model has better nonlinear feature recognition ability and more effective parameter optimization ability in small sample data set. The geothermal, biomass and other types of energy consumption in China have enriched the diversity of the energy supply structure and have experienced steady development in recent years. For example, biomass power generation has reached 52.9 billion kWh, which has increased 21.3% compared with that of last year.

4.6. Discussion

In contrast with PSO-GPR, GPR and ARIMA, the proposed MSTA-GPR displays a better forecasting result, owing to the effective parameter optimization of MSTA in hyper parameter selection for GPR. The forecasting outcomes reveal the changes of future energy consumption development in China. As obtained from the data in previous sections, the overall renewable energy consumption will grow at a mean rate of 8.25% during the thirteenth Five-Year Project, and the consumption of China's hydroelectricity will slightly grow at a mean rate of 1.60%. Additionally, the mean increase rate for China's wind power, solar power and geothermal, biomass and other types of energy consumption are 20.36%, 58.76% and 16.73%, respectively.

As far as we know, with the steady and rapid development of the economy, China's energy consumption will maintain a sustained growth momentum in the future. However, China's energy consumption system is still dominated by fossil fuels right now. The dependency on fossil fuel consumption is not sustainable, and serious environmental problems may occur owing to fossil fuel combustion, such as the greenhouse effect, acid rain, and others. China's renewable energy consumption will continue to grow at a steady speed, and the composition of the overall energy consumption will be more reasonable and balanced along with the application of corresponding energy policies. The prediction outcomes of this paper can offer useful information for the decision maker to foresee the future changes of renewable energy development and handle the environmental pollution problems, which can contribute for a smooth transition towards the 14th Five-Year Project and sustainable development in the future.

5. Conclusions

By integrating the modified state transition algorithm into Gaussian process regression, a novel approach MSTA-GPR is developed to make predictions more effective for China's renewable energy consumption. The main contribution of this article is to promote the forecasting performance of GPR with the application of MSTA in optimal hyper parameter selection. The superiority of MSTA in global optimization is validated with two well-known functions against the basic STA, GA and PSO. The suggested MSTA-GPR model is applied with the real data from 2008 to 2015 to make predictions of renewable energy consumption in China for the first three years of 13th Five-Year Project (2016–2020) to test the prediction performance.

The suggested approach can be easily applied and proved to be effective for short period prediction of time series. The forecasting outcomes reveal that compared with PSO-GPR, GPR and ARIMA, the MAPE of forecasting outcomes obtained by MSTA-GPR is superior to that of the other forecasting methods. This proves that the proposed MSTA-GPR is a better approach for renewable energy consumption and the forecasting performance of MSTA-GPR is better than hybrid model PSO-GPR, the basic GPR, and the traditional time series forecasting method ARIMA. Furthermore, the proposed MSTA-GPR approach is also supposed to deal with other complicated energy problems with various influence factors, for instance the price of electricity [46], solar radiation [47], and so on.

Author Contributions: L.Y. put forward the original idea in this paper and wrote the original manuscript; Y.J. and Y.D. offered the model technical support; Y.H. and C.G. reviewed and offered modification suggestions.

Funding: This investigation was funded by Baoding Low Carbon Economy Industry Research Institute Construction Project (2016BD0056).

Acknowledgments: The authors want to give thanks to the support of Baoding Low Carbon Economy Industry Research Institute Construction Project (2016BD0056).

Conflicts of Interest: The authors state that there is no conflict of interest.

Appendix A

Table A1. Consumption prediction for hydroelectricity of China from 2016 to 2018 (Mtoe).

Year	Real Data	MSTA-GPR		PSO-GPR		GPR		ARIMA	
		Value	Error (%)	Value	Error (%)	Value	Error (%)	Value	Error (%)
2016	260.96	260.96	0.00	257.65	1.27	261.97	0.39	267.82	2.63
2017	263.63	268.54	1.86	267.27	1.38	272.20	3.25	284.06	7.75
2018	272.08	272.08	0.00	272.08	0.00	277.34	1.93	300.58	10.47
MAPE			0.62		0.88		1.86		6.95

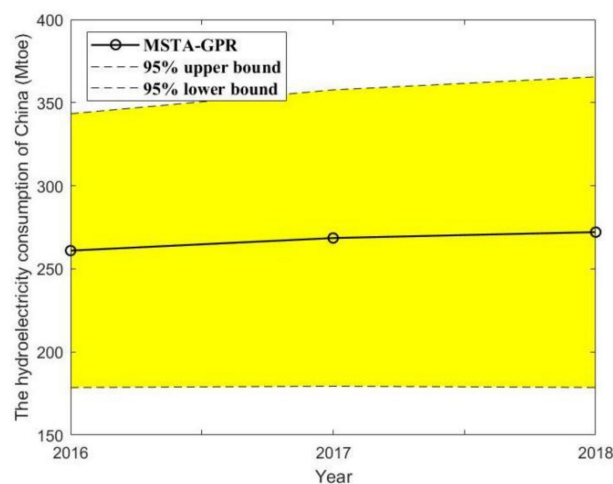


Figure A1. The interval prediction result of MSTA-GPR for China's hydroelectricity consumption.

Table A2. Wind power consumption data for China from 2016 to 2018 (Mtoe).

Year	Real Data	MSTA-GPR		PSO-GPR		GPR		ARIMA	
		Value	Error (%)	Value	Error (%)	Value	Error (%)	Value	Error (%)
2016	53.64	49.81	7.15	49.65	7.45	48.92	8.80	49.03	8.59
2017	66.75	61.32	8.14	60.79	8.94	59.59	10.74	56.28	15.69
2018	82.82	75.42	8.93	74.59	9.94	73.36	11.42	63.72	23.06
MAPE			8.07		8.77		10.32		15.78

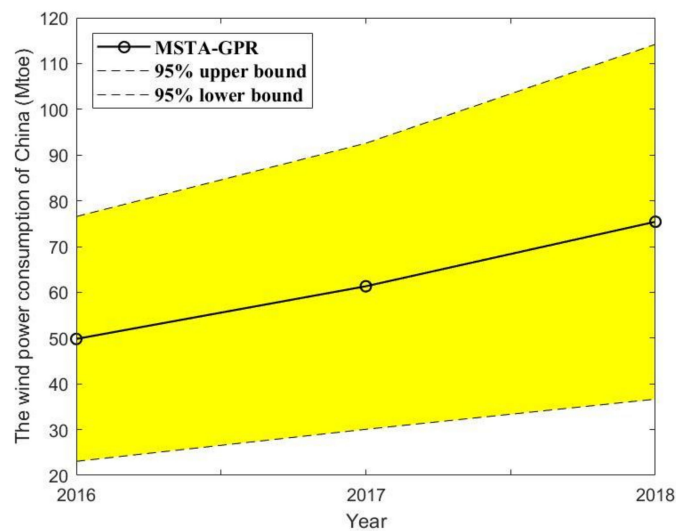


Figure A2. The interval prediction result of MSTA-GPR for China’s wind power consumption.

Table A3. Solar power consumption data for China from 2016 to 2018 (Mtoe).

Year	Real Data	MSTA-GPR		PSO-GPR		GPR		ARIMA	
		Value	Error (%)	Value	Error (%)	Value	Error (%)	Value	Error (%)
2016	13.96	15.40	10.36	15.47	10.84	16.71	19.72	14.60	4.62
2017	26.66	22.58	15.31	22.66	15.00	24.61	7.68	19.56	26.62
2018	40.16	40.16	0.00	40.16	0.00	43.88	9.26	24.73	38.44
MAPE			8.56		8.61		12.21		23.23

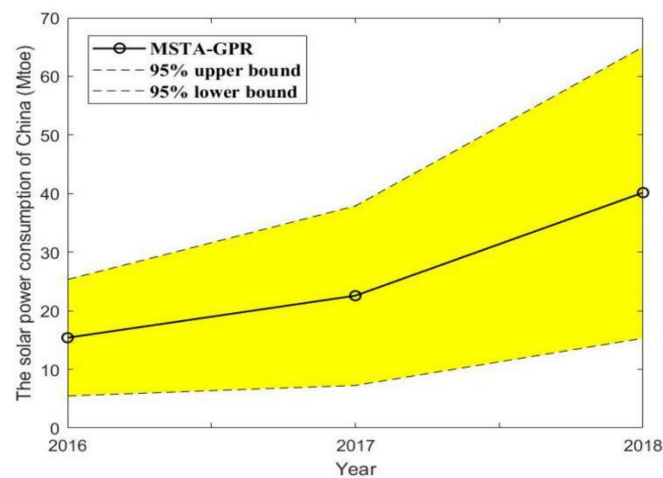
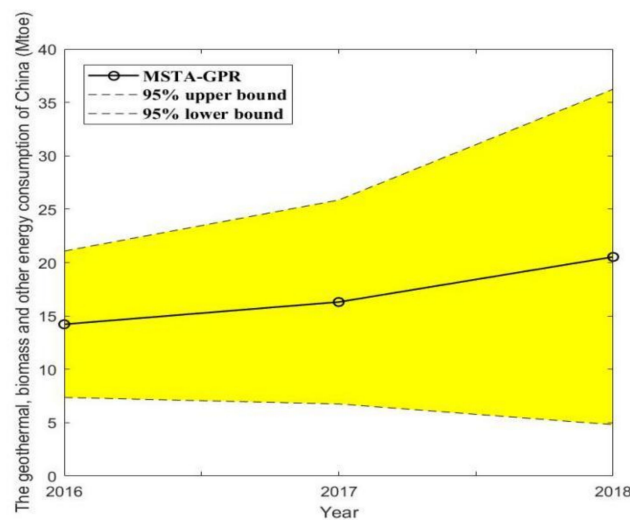


Figure A3. The interval prediction result of MSTA-GPR for China’s solar power consumption.

Table A4. Consumption prediction for geothermal, biomass and other energy from 2016 to 2018 (Mtoe).

Year	Real Data	MSTA-GPR		PSO-GPR		GPR		ARIMA	
		Value	Error (%)	Value	Error (%)	Value	Error (%)	Value	Error (%)
2016	14.06	14.22	1.13	14.08	0.17	14.36	2.13	13.88	1.28
2017	18.01	16.30	9.48	16.09	10.66	16.54	8.14	15.46	14.16
2018	20.53	20.53	0.00	20.53	0.00	21.18	3.19	16.99	17.22
MAPE			3.54		3.61		4.48		10.89

**Figure A4.** The interval prediction result of MSTAGPR for China's geothermal, biomass and other energy consumption.

References

- Divina, F.; Gilson, A.; Gómez-Vela, F.; García Torres, M.; Torres, J. Stacking ensemble learning for short-term electricity consumption forecasting. *Energies* **2018**, *11*, 949. [[CrossRef](#)]
- Pahle, M.; Pachauri, S.; Steinbacher, K. Can the Green Economy deliver it all? Experiences of renewable energy policies with socio-economic objectives. *Appl. Energy* **2016**, *179*, 1331–1341. [[CrossRef](#)]
- Singh, S.; Yassine, A. Big data mining of energy time series for behavioral analytics and energy consumption forecasting. *Energies* **2018**, *11*, 452. [[CrossRef](#)]
- Chang, Y.; Zheng, F.; Li, Y. Renewable energy policies in promoting financing and investment among the East Asia Summit countries: Quantitative assessment and policy implications. *Energy Policy* **2016**, *95*, 427–436. [[CrossRef](#)]
- Wang, Q. Effects of urbanisation on energy consumption in China. *Energy Policy* **2014**, *65*, 332–339. [[CrossRef](#)]
- Qiang, W.; Kan, Z. A framework for evaluating global national energy security. *Appl. Energy* **2017**, *188*, 19–31.
- Ang, B.W.; Choong, W.L.; Ng, T.S. A framework for evaluating Singapore's energy security. *Appl. Energy* **2015**, *148*, 314–325. [[CrossRef](#)]
- Bauer, N.; Mouratiadou, I.; Luderer, G.; Baumstark, L.; Brecha, R.J.; Edenhofer, O.; Kriegler, E. Global fossil energy markets and climate change mitigation—An analysis with REMIND. *Clim. Change* **2016**, *136*, 69–82. [[CrossRef](#)]
- Dirks, J.A.; Gorrissen, W.J.; Hathaway, J.H.; Skorski, D.C.; Scott, M.J.; Pulsipher, T.C.; Huang, M.; Ying, L.; Rice, J.S. Impacts of climate change on energy consumption and peak demand in buildings: A detailed regional approach. *Energy* **2015**, *79*, 20–32. [[CrossRef](#)]
- Dai, H.; Xie, X.; Yang, X.; Jian, L.; Masui, T. Green growth: The economic impacts of large-scale renewable energy development in China. *Appl. Energy* **2015**, *162*, 435–449. [[CrossRef](#)]
- Martínez-Álvarez, F.; Troncoso, A.; Riquelme, J. Recent Advances in Energy Time Series Forecasting. *Energies* **2017**, *10*, 809. [[CrossRef](#)]
- Schnaars, S.P. How to develop and use scenarios. *Long Range Plan.* **1987**, *20*, 105–114. [[CrossRef](#)]

13. Dong, K.Y.; Sun, R.J.; Li, H.; Jiang, H.D. A review of China's energy consumption structure and outlook based on a long-range energy alternatives modeling tool. *Pet. Sci.* **2017**, *14*, 214–227. [[CrossRef](#)]
14. Soroush, R.; Koochi, A.; Keivani, M.; Abadyan, M. A Bilayer Model for Incorporating the Coupled Effects of Surface Energy and Microstructure on the Electromechanical Stability of NEMS. *Int. J. Struct. Stab. Dyn.* **2017**, *17*, 1771005. [[CrossRef](#)]
15. Gabriel, S.A.; Kydes, A.S.; Whitman, P. The national energy modeling system: A large-scale energy-economic equilibrium model. *Oper. Res.* **2001**, *49*, 14–25. [[CrossRef](#)]
16. Meenal, R.; Selvakumar, A.I. Assessment of SVM, empirical and ANN based solar radiation prediction models with most influencing input parameters. *Renew. Energy* **2018**, *121*, 324–343. [[CrossRef](#)]
17. Cai, W.; Lai, K.H.; Liu, C.; Wei, F.; Ma, M.; Jia, S.; Jiang, Z.; Lv, L. Promoting sustainability of manufacturing industry through the lean energy-saving and emission-reduction strategy. *Sci. Total Environ.* **2019**, *665*, 23–32. [[CrossRef](#)]
18. Pei, D.; Wang, J.; Yang, W.; Tong, N. Multi-step ahead forecasting in electrical power system using a hybrid forecasting system. *Renew. Energy* **2018**, *122*, 533–550.
19. Rasmussen, C.E.; Nickisch, H. Gaussian Processes for Machine Learning (GPML) Toolbox. *J. Mach. Learn. Res.* **2010**, *11*, 3011–3015.
20. Jie, Y.; Chen, K.; Rashid, M.M. A Bayesian model averaging based multi-kernel Gaussian process regression framework for nonlinear state estimation and quality prediction of multiphase batch processes with transient dynamics and uncertainty. *Chem. Eng. Sci.* **2013**, *93*, 96–109.
21. Nair, R.; Jhingan, S.; Jain, D. Testing the consistency between cosmological measurements of distance and age. *Phys. Lett. B* **2015**, *745*, 64–68. [[CrossRef](#)]
22. Baraldi, P.; Mangili, F.; Zio, E. A belief function theory based approach to combining different representation of uncertainty in prognostics. *Inf. Sci.* **2015**, *303*, 134–149. [[CrossRef](#)]
23. Bogdan, M.; Brugger, D.; Rosenstiel, W.; Speiser, B. Estimation of diffusion coefficients from voltammetric signals by support vector and gaussian process regression. *J. Cheminform.* **2014**, *6*, 30. [[CrossRef](#)] [[PubMed](#)]
24. Chen, J.; Chan, L.L.T.; Cheng, Y.C. Gaussian process regression based optimal design of combustion systems using flame images. *Appl. Energy* **2013**, *111*, 153–160. [[CrossRef](#)]
25. Peng, K.; Feng, G.; Guan, X. Sparse online warped Gaussian process for wind power probabilistic forecasting. *Appl. Energy* **2013**, *108*, 410–428.
26. Wang, J.; Hu, J. A robust combination approach for short-term wind speed forecasting and analysis—Combination of the ARIMA (Autoregressive Integrated Moving Average), ELM (Extreme Learning Machine), SVM (Support Vector Machine) and LSSVM (Least Square SVM) forecasts us. *Energy* **2015**, *93*, 41–56. [[CrossRef](#)]
27. He, Z.K.; Liu, G.B.; Zhao, X.J.; Wang, M.H. Overview of Gaussian process regression. *Control Decis.* **2013**, *28*, 1121–1129.
28. Xiong, Z.H.; Huang, G.H.; Shao, H.H. Comparison and Application Research on Soft Sensor Modeling Based on Gaussian Processes and Support Vector Machines. *Inf. Control* **2004**, *33*, 754–757.
29. Liu, K.; Liu, B.; Chong, X.U. Intelligent analysis model of slope nonlinear displacement time series based on genetic-gaussian process regression algorithm of combined kernel function. *Chin. J. Rock Mech. Eng.* **2009**, *28*, 2128–2134.
30. Yu, S.; Ke, W.; Wei, Y.M. A hybrid self-adaptive Particle Swarm Optimization–Genetic Algorithm–Radial Basis Function model for annual electricity demand prediction. *Energy Convers. Manag.* **2015**, *91*, 176–185. [[CrossRef](#)]
31. Rahmani, R.; Yusof, R.; Seyedmahmoudian, M.; Mekhilef, S. Hybrid technique of ant colony and particle swarm optimization for short term wind energy forecasting. *J. Wind Eng. Ind. Aerodyn.* **2013**, *123*, 163–170. [[CrossRef](#)]
32. Bahrami, S.; Hooshmand, R.A.; Parastegari, M. Short term electric load forecasting by wavelet transform and grey model improved by PSO (particle swarm optimization) algorithm. *Energy* **2014**, *72*, 434–442. [[CrossRef](#)]
33. Hui, L.; Tian, H.; Liang, X.; Li, Y. New wind speed forecasting approaches using fast ensemble empirical model decomposition, genetic algorithm, Mind Evolutionary Algorithm and Artificial Neural Networks. *Renew. Energy* **2015**, *83*, 1066–1075.

34. Hui, L.; Tian, H.Q.; Chao, C.; Li, Y.F. An experimental investigation of two Wavelet-MLP hybrid frameworks for wind speed prediction using GA and PSO optimization. *Int. J. Electr. Power Energy Syst.* **2013**, *52*, 161–173.
35. Da, L.; Niu, D.; Hui, W.; Fan, L. Short-term wind speed forecasting using wavelet transform and support vector machines optimized by genetic algorithm. *Renew. Energy* **2014**, *62*, 592–597.
36. Miao, H.; Zhou, X.; Huang, T.; Yang, C.; Gui, W. Dynamic optimization based on state transition algorithm for copper removal process. *Neural Comput. Appl.* **2017**, *31*, 2827–2839.
37. Rasmussen, C.E.; Williams, C.K.I. *Gaussian Processes for Machine Learning (Adaptive Computation and Machine Learning)*; The MIT Press: Cambridge, MA, USA, 2005; pp. 69–106.
38. Fang, D.; Zhang, X.; Yu, Q.; Jin, T.C.; Tian, L. A novel method for carbon dioxide emission forecasting based on improved Gaussian processes regression. *J. Clean. Prod.* **2018**, *173*, 143–150. [[CrossRef](#)]
39. Zhou, X.; Yang, C.; Gui, W. Nonlinear system identification and control using state transition algorithm. *Appl. Math. Comput.* **2014**, *226*, 169–179. [[CrossRef](#)]
40. Zhou, X.; Yang, C.; Gui, W. A Statistical Study on Parameter Selection of Operators in Continuous State Transition Algorithm. *IEEE Trans. Cybern.* **2019**, *49*, 3722–3730. [[CrossRef](#)]
41. Tran, T.D.; Jin, G.G. Real-coded genetic algorithm benchmarked on noiseless black-box optimization testbed. In Proceedings of the 12th Annual Conference Companion on Genetic and Evolutionary Computation, Portland, OR, USA, 7–11 July 2010; ACM: New York, NY, USA, 2010; pp. 1731–1738.
42. Iadevaia, S.; Lu, Y.; Morales, F.C.; Mills, G.B.; Ram, P.T. Identification of optimal drug combinations targeting cellular networks: Integrating phospho-proteomics and computational network analysis. *Cancer Res.* **2010**, *70*, 6704–6714. [[CrossRef](#)]
43. Guo, J.; Chen, F.; Xu, C. Traffic Flow Forecasting for Road Tunnel Using PSO-GPR Algorithm with Combined Kernel Function. *Math. Probl. Eng.* **2017**, *2017*, 2090783. [[CrossRef](#)]
44. Gao, W.; Karbasi, M.; Hasanipanah, M.; Zhang, X.; Guo, J. Developing GPR model for forecasting the rock fragmentation in surface mines. *Eng. Comput.* **2018**, *34*, 339–345.
45. Karmy, J.P.; Maldonado, S. Hierarchical Time Series Forecasting via Support Vector Regression in the European Travel Retail Industry. *Expert Syst. Appl.* **2019**, *137*, 59–73. [[CrossRef](#)]
46. Yang, W.; Wang, J.; Niu, T.; Du, P. A hybrid forecasting system based on a dual decomposition strategy and multi-objective optimization for electricity price forecasting. *Appl. Energy* **2019**, *235*, 1205–1225. [[CrossRef](#)]
47. Fan, J.; Wu, L.; Zhang, F.; Cai, H.; Zeng, W.; Wang, X.; Zou, H. Empirical and machine learning models for predicting daily global solar radiation from sunshine duration: A review and case study in China. *Renew. Sustain. Energy Rev.* **2019**, *100*, 186–212. [[CrossRef](#)]

